Supplementary Information for:

Electron-Phonon Coupling and Symmetry-Breaking in Superconducting Oxide Interfaces Near Ferroelectric Quantum Criticality

Roger Guzman[1*+], Miguel Pruneda[2,3*], Jean Paul Nery[4,5], Mingquan Xu[1], Aowen Li[1], Nils Wittemeier[3], Ang Li[1], Gyanendra Singh[4], Nicolas Bergeal[6], Alexei Kalaboukhov[7], Gervasi Herranz[4*], Jaume Gazquez[4], Wu Zhou[1*]

1. School of Physical Sciences, University of Chinese Academy of Sciences, Beijing, China.
2. Nanomaterials and Nanotechnology Research Center (CINN), CSIC-UNIOVI, El Entrego, Asturias, Spain.
3. Catalan Institute of Nanoscience and Nanotechnology (ICN2), CSIC and BIST, Bellaterra, Barcelona, Spain.
4. Institute of Materials Science of Barcelona (ICMAB-CSIC), Bellaterra, Barcelona, Spain.
5. Nanomat Group, QMAT Research Unit, and European Theoretical Spectroscopy Facility, Université de Liège, B-4000 Liège, Belgium
6. Laboratoire de Physique et d'Etude des Matériaux, ESPCI Paris, Université PSL, CNRS, Sorbonne Université, Paris, France.
7. Department of Microtechnology and Nanoscience - MC2, Chalmers University of Technology, Gothenburg, Sweden

*Corresponding authors:
rguzman@icmab.es, mpruneda@csic.es, gherranz@icmab.es, wuzhou@ucas.ac.cn
[+]Current address:
Institute of Materials Science of Barcelona (ICMAB-CSIC), Bellaterra, Barcelona, Spain.

Supplementary Note 1. Vibrational EELS

The phonon EELS spectra of LAO/STO interfaces show mainly five peaks, P1-P5, which are assigned as respect to the bulk phonon modes of cubic STO for simplicity[1–4] (**Extended Data Fig. 2-3**). The P5 peak (~99 meV) is assigned to the LO4 mode with predominantly oxygen vibrations; P4-P3 peaks to TO4/LO3 (~62 meV) and TO3/LO2 (~45 meV), respectively, comprising vibrations of Ti and oxygen atoms; P2 peak to TO2/LO1 (~32 meV) modes with Ti, O and Sr vibrations; P1 peak (~19 meV) is assigned to a mixture of acoustic modes ascribed to Sr vibrations.

As discussed in the main text, the vibrational response of the LAO/STO interfaces show an evolution in peaks intensities and phonon frequencies with the increase in interfacial charge density (i.e., from sample S1 to S4). In general, we observe a systematic blueshift of the STO bulk phonon modes towards the interface plane (Ti_0) along with a decrease in peaks intensities when crossing the 2DEG. An exception is the highest frequency longitudinal optical phonon mode of STO, the LO4 (P5), which exhibits a distinct response to the electron phonon interaction (EPI). When crossing the bottom interface of the 2DEG, the LO4 peak gradually blueshifts reaching a maximum value of ~102 meV, followed by a redshift as it approaches the interface Ti_0 in the case of low doping interfaces. The maxima are indicated by red arrows in the detailed profiles of the energy shift of the LO4 mode in **Fig. S1a**. The kink in the LO4 energy marks a sub-interface within the 2DEG region (green shaded area) and is located at ~Ti_3 distance in samples S1, ~Ti_4 in samples S2-S3 (red arrows). However, the redshift of LO4 near Ti_0 decrease with charge doping, and we observe a crossover for the highest doping sample S4 in which the LO4 will remain hard at a fairly constant value within the 2DEG.

Theoretical calculations of the phonon dispersion for cubic STO predicts softening of the LO4 upon increasing electron doping[5]. Although we clearly observe this behavior in the case of low-doping samples, the hard LO4 in high-doping samples is at odds with current calculations. In view of these observations, we speculate that the observed hard LO4 phonon for high-doping samples may be due to the coupling to plasmons. It is sometimes assumed that additional screening gives rise to a reduced LO frequency due to reduced LO-TO splitting. However, the coupling between the plasmon and LO modes give rise to a mixed LO-plasmon quasiparticle that has a higher frequency, as has been well established long ago both theoretically[6], and in Raman[7] and infrared experiments[8]. More recently, high-resolution EELS experiments have observed LO-plasmon peaks in FeSe/STO[10] and also CoSe/STO[11] at frequencies much larger than LO4, referred to as "polaronic plasmons". The LO-plasmon coupling has also been observed through "plasmonic polarons" in ARPES

experiments, where the distance from a satellite to the main quasiparticle peak is larger than the LO4 frequency[8,9]. The role of plasmons is sometimes disregarded based on the assumption that they do not couple with phonons and due to the lack of frequency shifts, within experimental error, proportional to the square root of the density. However, at low doping, the character of the LO-plasmon is mostly phonon-like and the increase of the frequency is very small. Thus, we believe the unexplained origin of the 118 meV satellite in Cancellieri et al. (ref [4]) may originate from the LO-plasmon coupling. Based on these observations, we tentatively attribute the increase in LO4 frequency with charge density to its coupling with plasmons. In bulk 3D doped systems, this effect is more pronounced suggesting that the limited spatial extent of the 2DEG at the highly doped interface leads to only mild frequency hardening. Calculations that include phonon-plasmon coupling are likely necessary to account for all effects in these LAO/STO systems, but are probably beyond reach of first-principles methods.

In agreement with calculations of bulk STO in Cancellieri et al. (ref [5]), our calculations of LAO/STO heterostructures show a similar trend with doping in which the LO4 mode softens near the interface, which suggests the observed phenomenon may be a combination of both interfacial and doping effects. We elaborated a qualitative model to describe the interplay between the plasmon and LO4 mode at the interface. **Fig. S1b** shows a schematic of the experimental curves, in green, of the experimental curves. The blue curve corresponds to a hypothetical system of bulk STO with a 2DEG close to z=0. Due to the LO-plasmon coupling, the frequency of LO4 is maximum at z=0, where the concentration of electrons is higher, and decreases to the bulk value far from z=0. The orange curve represents an LAO/STO system without a 2DEG: in this case, the frequency gradually shifts from the bulk STO value to the bulk LAO value (the highest mode in both crystals corresponds to the same vibration pattern). The width of the transition depends on how much the LAO and STO deform close to the interface (this assumes a smooth transition and does not take into account a sharp discontinuity in the lattice constant, which gives rise to the very localized LVM). The green curve, at z>0, is just the average of the blue and orange curves, which have compensating effects: while the 2DEG would make the frequency increase at z=0, the lower LAO frequency makes it decrease. Thus, the maximum value would be located at some finite STO layer. At z<0, the curve decreases towards the bulk LAO frequency. In the samples, to the right, LO4 reaches the bulk STO value. But to the left, there is a small number of LAO layers, so there are also interface and surface effects.

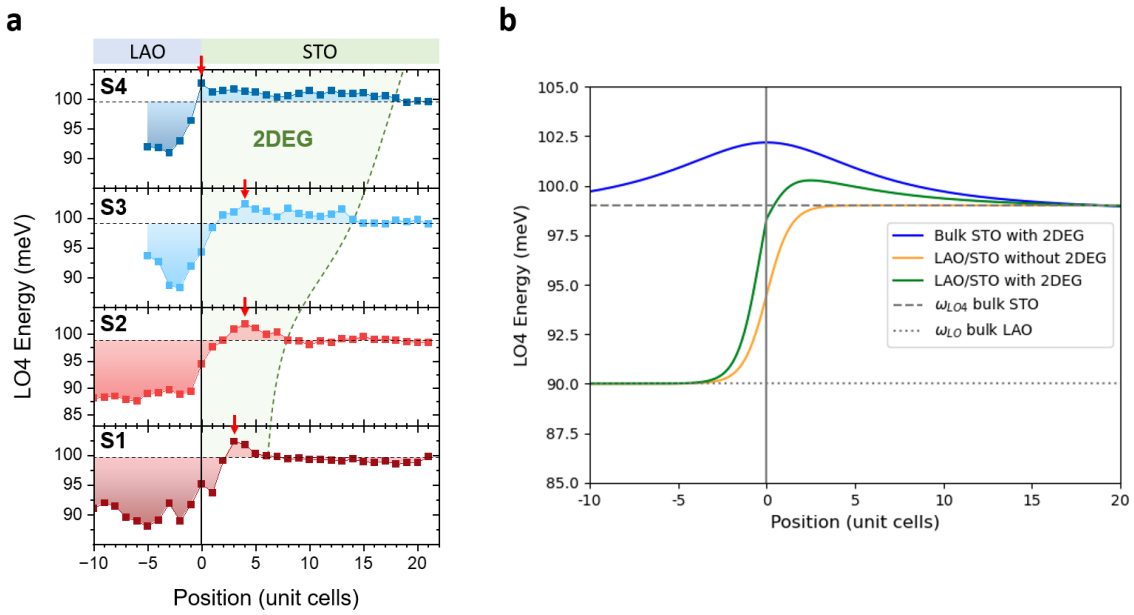

Fig. S1. Response of the LO4 phonon mode to interfacial charge doping. a, profiles in the energy range of the LO4 mode for samples S1-S4. The green shaded area delimitates the spatial extension of the 2DEG. Vertical red arrows indicate the energy maxima of the LO4 mode in samples S1-S4. **b,** Schematic qualitative model representing the plasmon-LO4 coupling occurring at the LAOS/STO interface.

Supplementary Note 2. Calculation of the electron-phonon coupling with finite differences

From finite differences on the Hamiltonian in real space, we extract the electron-phonon vertex in our supercell:

$$g_{mn,\upsilon}(k,q) = \sum_{i,\alpha\beta,RR'} (u_{qi}^{\upsilon}) \cdot e^{-i(k+q)\cdot R} \cdot e^{+ik\cdot R'} \cdot c_{m\alpha}^{\dagger}(k+q) \cdot c_{n\beta}(k) \cdot \left[\partial_{i0} H_{\alpha\beta}(R,R') - \sum_{\gamma\mu} \left(\partial_{i0} S_{\alpha\mu}(R,R') S_{\mu\gamma}^{-1}(k) H_{\gamma\beta}(k) - H_{\alpha\mu}(k) S_{\mu\gamma}^{-1}(k) \partial_{i0} S_{\gamma\beta}(R,R') \right) \right]$$

where $H_{\alpha\beta}(R,R') = \langle \phi_\alpha(R) | H | \phi_\beta(R') \rangle$ and $S_{\alpha\beta}(R,R') = \langle \phi_\alpha(R) | \phi_\beta(R') \rangle$ denote the Hamiltonian and Overlap matrices in the basis of atomic orbitals centered at cells R and R', $c_{n\alpha}(k)$ are the coefficients of the electronic wavefunctions in that basis: $\psi_{nk}(r) = \sum_{\alpha R} \left[e^{ik\cdot R} \cdot c_{n\alpha}(k) \cdot \phi_\alpha(r-R) \right]$. $A_{\alpha\beta}(k)$ is the Fourier transform of the matrix to k-space and $\partial_{i0} A_{\alpha\beta}$ denotes its change due to the displacement of atom "i" in reference unit cell "0". Finally, u_{qi}^{υ} is the displacement vector for each atom following the phonon mode (υ, q). In our simulation we took a unit cell corresponding to the slab geometry with 120 atoms (6 layers of $SrTiO_3$ and 6 layers of $LaAlO_3$, oriented along the 001 direction, **Fig. S2**), and built a 3x3x1 supercell (1080 atoms). The force constant matrix, and derivatives of Hamiltonian and Overlap were computed from atomic displacements of all atoms within the supercell. Assuming locality in the perturbation, this "real space description" allows to subsequently extract an arbitrary sampling of the dynamical matrix and the e-ph vertex in reciprocal space, as done in Wannier interpolation schemes. More details of this implementation will be given elsewhere. Note that in our calculation we are not including long-range dipolar nor quadrupolar interactions, which might dominate for some specific phonon modes for $q \to 0$. In particular, the Fröhlich term will give a significant contribution for the in-plane local modes identified at ~70-80 meV. Considering that in our system the interface breaks periodicity, the local description of out-of-plane local modes seems reasonable.

The electron-phonon coupling strength is given by

$$\lambda_{q\upsilon} = \frac{2}{\omega_{q\upsilon} N(\varepsilon_F)} \sum_{nm} \int_{BZ} \frac{dk}{\Omega_{BZ}} |g_{mn,\upsilon(k,q)}|^2 \delta(\varepsilon_{nk} - \varepsilon_F) \delta(\varepsilon_{mk+q} - \varepsilon_F)$$

where $N(\varepsilon_F)$ is the density of states at the Fermi level. From λ_{qv} we can obtain the phonon linewidths $\gamma_{qv} \sim \omega_{qv}^2 \cdot \lambda_{qv}$.

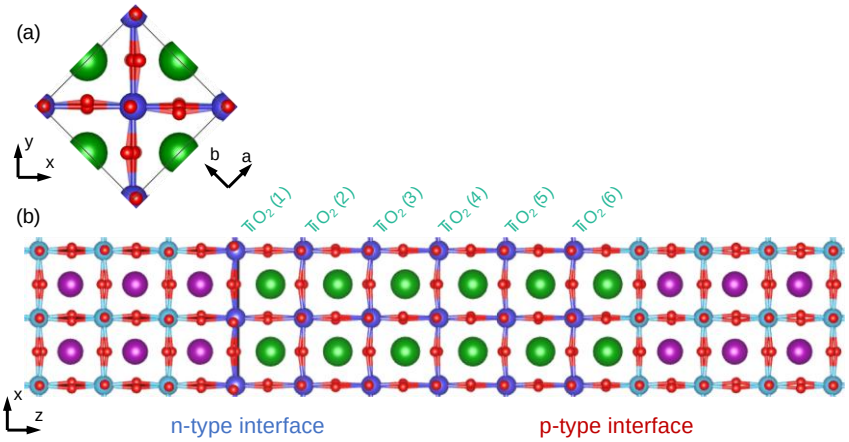

Fig. S2. Model atomic structure used for the LAO/STO superlattice. The stoichiometric supercell contains two interfaces (n-type and p-type) between $LaAlO_3$ and $SrTiO_3$. The in-plane cell is $\sqrt{2} \times \sqrt{2}$ of the pseudocubic lattice (top view in panel a), and compatible with the rhombohedral $LaAlO_3$ phase. The TiO_2 atomic layers are numbered from the n-type interface where the 2DEG is localized (side view in b).

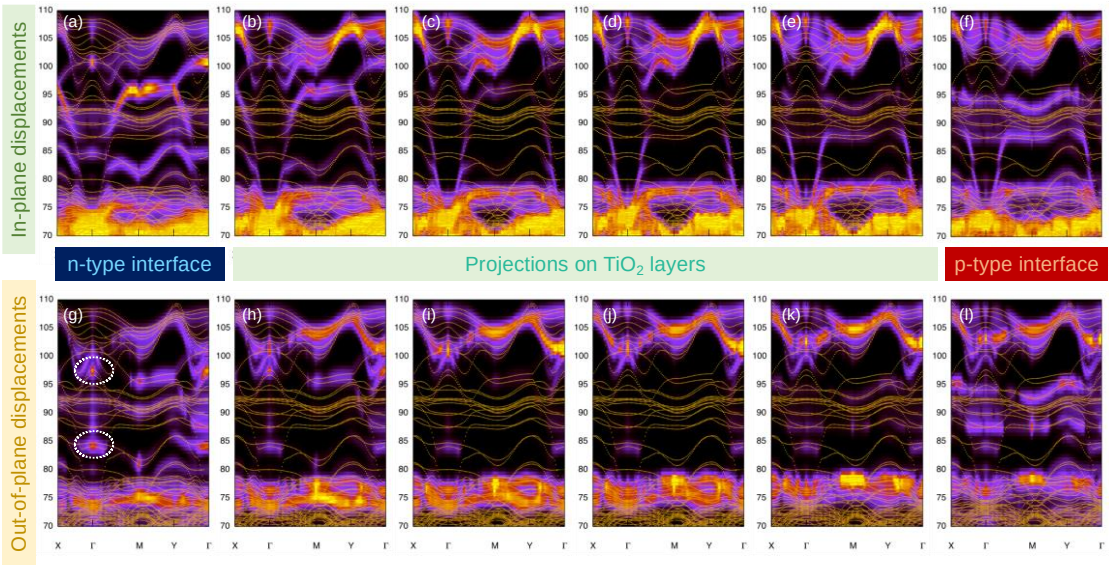

Fig. S3. Phonon band structures (fatbands) projected on different atomic layers through the $SrTiO_3$ slab in the LAO/STO heterostructure with 0.1e/cell. Contributions of in-plane atomic displacements for TiO2(1)-TiO2(6) layers are shown in panels (a) to (f). Out-of-plane displacements are shown in (g) to (l). Brighter colors correspond to larger displacements of the

atoms in that atomic layer. TiO2 layer close to the LAO interface at the n-type (a, g) and p-type interfaces (f, l) show local vibrational modes that are absent in the central (bulk-like) layers. Panel (g) highlights two out-of-plane vibrational modes that correspond to oxygen displacements in the nearby LaO layer (white circle at ~85meV) or the SrO layer (circle at ~97meV, corresponding to the mode shown in Fig. 4e in the main text).

REFERENCES

1. Nucara, A. *et al.* Hardening of the soft phonon in bulk $SrTiO_3$ interfaced with $LaAlO_3$ and $SrRuO_3$. *Phys. Rev. B* **93**, 224103 (2016).
2. Yan, X. *et al.* Real-space visualization of frequency-dependent anisotropy of atomic vibrations. *arXiv:2312.01694* (2023).
3. Yang, H. *et al.* Phonon modes and electron–phonon coupling at the FeSe/$SrTiO_3$ interface. *Nature* **635**, 332–336 (2024).
4. Vogt, H. Hyper-Raman tensors of the zone-center optical phonons in $SrTiO_3$ and $KTaO_3$. *Phys. Rev. B* **38**, 5699 (1988).
5. Cancellieri, C. *et al.* Polaronic metal state at the $LaAlO_3$/$SrTiO_3$ interface. *Nat. Commun.* **7**, 10386 (2016).
6. Varga, B. B. Coupling of plasmons to polar phonons in degenerate semiconductors. *Phys. Rev.* **137**, A1896 (1965).
7. Mooradian, A. & Wright, G. B. Observation of the interaction of plasmons with longitudinal optical phonons in GaAs. *Phys. Rev. Lett.* **16**, 999 (1966).
8. Olson, C. G. & Lynch, D. W. Longitudinal-optical-phonon-plasmon coupling in GaAs. *Phys. Rev.* **177**, 1231 (1969).